Chinese Chemical Letters 35 (2024) 108573

Contents lists available at ScienceDirect

Chinese Chemical Letters

journal homepage: www.elsevier.com/locate/cclet

# Surface engineering of carbon dots for highly sensitive $\alpha$-glucosidase assay and inhibition evaluation

Meijuan Liang[a,b,1], Gege Song[a,1], Yeqing Wan[a], Yingying Chen[a], Fuan Wang[a,*], Xiaoqing Liu[a,*]

[a] College of Chemistry and Molecular Sciences, Wuhan University, Wuhan 430072, China
[b] Oil Crops Research Institute, Chinese Academy of Agricultural Sciences, Wuhan 430062, China

ARTICLE INFO

*Article history:*
Received 17 January 2023
Revised 25 April 2023
Accepted 15 May 2023
Available online 19 May 2023

*Keywords:*
$\alpha$-Glucosidase
Carbon dots
Fluorescent sensor
Inhibitor
$\beta$-Cyclodextrin

ABSTRACT

Monitoring $\alpha$-glucosidase ($\alpha$-Glu) activity is of great significance for the early diagnosis of type II diabetes. Here the blue fluorescent carbon dots (CDs) were integrated with two different recognizing molecules, $\beta$-cyclodextrin and phenylboronic acid, for assembling a multifunctional CDs (mCDs) nanoplatform for sensitively analyzing $\alpha$-Glu and its inhibitors. The hydrolyzed product of 4-nitrophenyl-$\alpha$-D-glucopyranoside ($\alpha$-Glu substrate), *p*-nitrophenol, could efficiently quench the fluorescence of mCDs due to its cooperative molecular recognition with $\beta$-cyclodextrin and phenylboronic acid. The mCDs could be utilized for the detection of $\alpha$-Glu activity with the limit of detection of 0.030 U/L. Moreover, the present $\alpha$-Glu detection platform revealed a high selectivity, and other natural enzymes showed scarcely any effect on the present mCDs system. The proposed method could be facilely used to screen $\alpha$-Glu inhibitors with satisfying performance. The rational mCDs is expected to supplement more comprehensive biosensing platforms for highly sensitive and specific recognition of disease-relevant biomarkers with clinical importance.



Diabetes mellitus is a serious and chronic public disease, and the accompanying nephropathy, retinopathy, neuropathy, ulceration, and cardiovascular diseases, always bring inconvenient and even fatal threats for diabetes patients [1,2]. International Diabetes Federation has reported that 537 million adults suffered from diabetes, and has also predicted that the worldwide diabetic cases will increase to 783 million by 2045 [3]. Among these diabetes cases, more than 90% of cases are type II insulin-irrelative diabetes mellitus [4]. As a well-known biomarker of type II diabetes locating at the epithelium of small intestine, $\alpha$-glucosidase ($\alpha$-Glu) could hydrolyze $\alpha$-glucopyranoside to release glucose, resulting in a high expression level of blood glucose after a meal [5,6]. In the early treatment and prevention of type II diabetes, $\alpha$-Glu inhibitors have been identified as effective drugs for blocking the digestion of carbohydrates and the subsequent absorption of glucose in small intestine [7]. Therefore, the monitoring of $\alpha$-Glu activity and the screening of $\alpha$-Glu inhibitors have a significant implication for the accurate diagnosis and effective prevention of diabetes.

Recently, luminescent carbon dots (CDs) have attracted much attention in biosensing researches due to their predominant advantages of high resistance to photobleaching, excellent biocompatibility and low toxicity [8–10]. CDs could inherit the high affinity of their precursors toward the corresponding targets *via* the surface-decorated recognition groups. Thus these as-achieved functional CDs could be facilely utilized as ideal sensing candidates for specific target recognition and detection [11–13]. In order to achieve diverse functionalities, the surface of CDs requires more extensive modifications with distinct ligands. Up to date, the functionalized CDs were always obtained through the one-pot synthesis from recognition sites-involved precursors, or the post-synthetic chemical conjugation of recognition molecules onto CDs surfaces. For instance, by using boric acid as recognition group, CDs could be conveniently utilized for selective discrimination of $\alpha$-Glu and its inhibitors [14]. However, this chemical conjugation strategy requires multistep preparation, and leads to poor reproducibility. Then the synthesis of $\alpha$-Glu targeting CDs was achieved *via* the simplified one-pot hydrothermal preparation from 3-aminobenzeneboronic acid and 1,2-ethylenediamine precursors [15]. However, these boric acid-modified CDs are still confronted with limited sensitivity and specificity for $\alpha$-Glu assay. Thus, it is highly desirable to develop a

* Corresponding authors.
*E-mail addresses:* fuanwang@whu.edu.cn (F. Wang), xiaoqingliu@whu.edu.cn (X. Liu).
[1] These authors contributed equally to this work.

https://doi.org/10.1016/j.cclet.2023.108573
1001-8417/

facile and more accessible CDs-based $\alpha$-Glu sensing platform with improved sensitivity and efficiency.

$\beta$-Cyclodextrin, a well-known molecular host, can selectively accommodate organic molecules into its hydrophobic cavity *via* the specific guest/host association interaction. $\beta$-Cyclodextrin has recently been modified onto the surface of luminescent quantum dots for selective and sensitive sensing purpose [16–18]. Meanwhile, $\beta$-cyclodextrin-derived CDs have also emerged as a versatile means for the detection of different metal ions, amino acids, and proteins [19–21]. We anticipated that the simultaneous functionalization of CDs with combination of boric acid and $\beta$-cyclodextrin could realize a substantially enhanced detection of $\alpha$-Glu and its inhibitors *via* the cooperative recognition from their multiple distinct sensing mechanism fronts. Herein, the multifunctional CDs (mCDs) were constructed by using phenylboronic acid and $\beta$-cyclodextrin as precursors *via* one-pot solvothermal method. The as-achieved mCDs showed highly specific and sensitive detection of $\alpha$-Glu through the surface-anchored boronic acid and $\beta$-cyclodextrin recognizing groups. *p*-Nitrophenol (NP), the hydrolysis product of $\alpha$-Glu substrate, could simultaneously bind with boronic acid and accommodate into $\beta$-cyclodextrin cavity of mCDs for quenching its fluorescence (Scheme 1). The NP-mediated quenching principle of mCDs was systematically investigated toward sensitive $\alpha$-Glu detection. Besides, the mCDs/$\alpha$-Glu system could be utilized to efficiently detect $\alpha$-Glu inhibitors with high sensitivity. Accordingly, the rational engineering of multiple recognition sites on mCDs has supplemented a versatile and robust sensing platform for the detection of $\alpha$-Glu and for the screening of its inhibitors, and thus shows great promise for clinical diagnosis and treatment.

The bright blue fluorescent mCDs were facilely assembled through the facile solvothermal treatment of $\beta$-cyclodextrin and phenylboronic acid mixture. Meanwhile, to reveal the function of $\beta$-cyclodextrin and phenylboronic acid precursor, $\beta$-cyclodextrin-absent (pCDs) and phenylboronic acid-absent ($\beta$CDs) CDs were synthesized from only phenylboronic acid and $\beta$-cyclodextrin precursor (Fig. 1A). The as-prepared mCDs revealed a uniformly spherical nanostructure with an average diameter of 2.2 nm, which was slightly smaller than that of $\beta$CDs (2.6 nm) and pCDs (2.4 nm, Fig. 1B and Fig. S1 in Supporting information). The chemical compositions of these different CDs were subsequently analyzed by X-ray photoelectron spectroscopy (XPS, Fig. 1C), which revealed the representative peaks of C, N, O, and B elements. The high-resolution XPS analysis of B 1s from mCDs was deconvoluted into two peaks for C−B (191.8 eV) and B−O (192.7 eV, Fig. S2A in Supporting information) [22]. For XPS analysis of surface C 1s of mCDs, the peaks at 283.9, 284.4, 285.7, 286.4, and 287.7 eV were denoted to the C−B, C=C/C−C, C−N, C−O and C=O groups, respectively (Fig. S2B in Supporting information) [23–25]. The XPS analysis of N 1s showed two different peaks at 400.2 and 401.7 eV, which corresponded to the form of C−N and N−H bonds in the generated mCDs (Fig. S2C in Supporting information) [26]. The XPS analysis

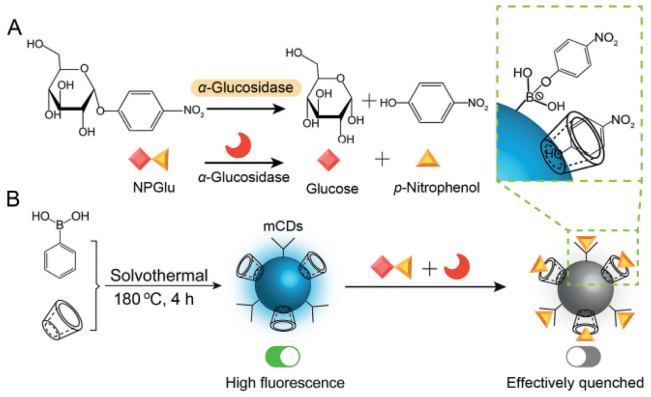


**Scheme 1.** Schematic illustration of the sensing mechanism of $\alpha$-Glu assay. (A) $\alpha$-Glu catalyzed hydrolysis of 4-nitrophenyl-$\alpha$-D-glucopyranoside (NPGlu) substrate. (B) The principle of mCDs derived form $\beta$-cyclodextrin/phenylboronic acid for $\alpha$-Glu assay.

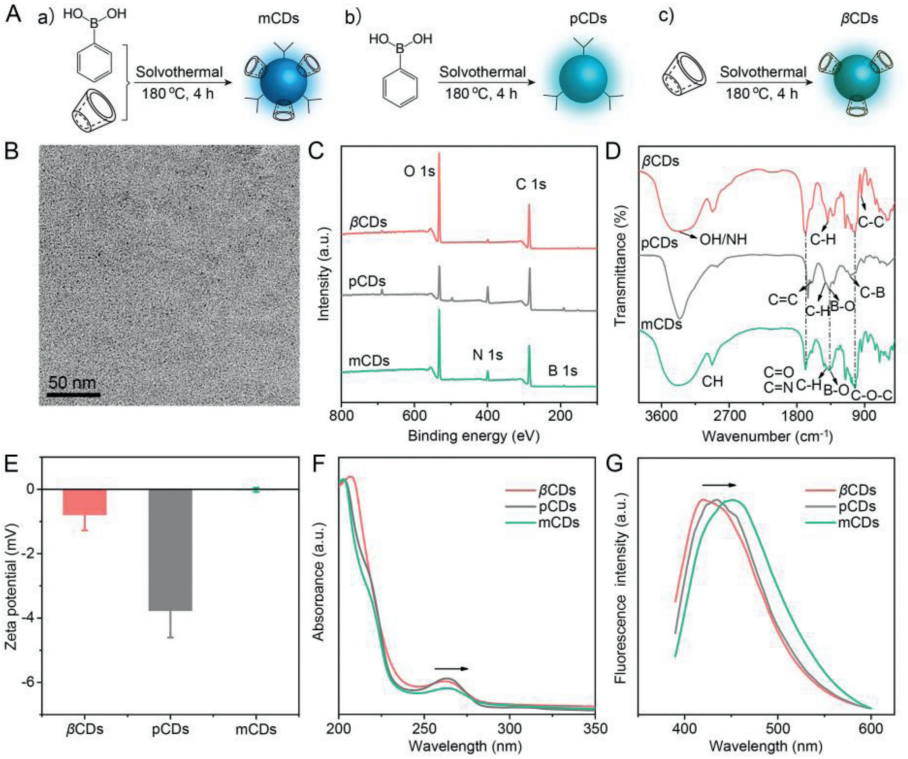


**Fig. 1.** Characterization of the multifunctional CDs. (A) The synthesis of (a) mCDs, (b) pCDs and (c) $\beta$CDs. (B) TEM image, (C) XPS survey spectra, (D) FTIR characterization, (E) zeta potential, (F) UV–vis absorption, and (G) fluorescence spectra of these differently prepared CDs with the same excitation of 370 nm.

of O 1s revealed three different peaks at 530.9, 531.6 and 533.2 eV, which indicated the formation of C=O, C−O−C/C−OH and B–O for the obtained mCDs, respectively (Fig. S2D in Supporting information) [16,27]. Particularly, in comparison with $\beta$CDs and pCDs control, the newly introduced C−B and C−O bonds, together with the obviously shifted XPS peaks of C and O, indicated the varied chemical composite of mCDs by $\beta$-cyclodextrin and phenylboronic acid. Besides, Fourier transform infrared (FTIR) spectroscopy was employed to characterize these CDs. As revealed in Fig. 1D, the broad absorbance of 3500–3000 $cm^{-1}$ was attributed to the stretching vibrations of −OH and −NH bonds, while the peak at 1680 $cm^{-1}$ suggested the existence of C=O and C=C stretching vibration [28]. These peaks between 2980 and 2860 $cm^{-1}$ were assigned to the C−H stretching vibration of methyl/methylene groups. The peak of mCDs at 1343 $cm^{-1}$ could be attributed to the stretching vibration of B−O bond [22], which was similar to that of $\beta$CDs and pCDs control. Similarly, C−N/C=N stretching vibration, N−H deformation vibration, and the C=O stretching of amine bond was observed at 830, 1640 and 1240 $cm^{-1}$, respectively [29–31]. Furthermore, zeta potential was performed to investigate the surface charge of these CDs. As compared to the negatively charged $\beta$CDs (−0.791 mV) and pCDs (−3.77 mV), mCDs showed less negative charge (−0.016 mV, Fig. 1E), indicating that the compact mCDs were simultaneously functionalized with phenylboronic acid and $\beta$-cyclodextrin.

Having demonstrated the successful construction of mCDs, the optical property of mCDs was then investigated *via* UV–vis absorption and fluorescence spectroscopy. The UV–vis absorption of mCDs showed two typical absorption bands at 220 nm and 265 nm (Fig. 1F), which was ascribed to the $\pi$-$\pi^*$ transition of aromatic $sp^2$ domain and the $n$-$\pi^*$ electron of C=O bond, respectively [32]. Note that the characteristic peaks of mCDs at 265 nm exhibited a red-shift absorption from 260 nm to 265 nm in relative to that of $\beta$CDs (261 nm) and pCDs (263 nm), demonstrating the existence of $\beta$-cyclodextrin and phenylboronic acid in the compact mCDs. Then the detailed photoluminescence property of mCDs was performed under various excitation wavelengths. It showed that mCDs presented an excitation-tunable luminescence behavior (Fig. S3 in Supporting information). The excitation-dependent fluorescence of mCDs can be attributed to the quantum confinement of conjugated $\pi$-electrons in a $sp^2$ network, the surface defects (including heteroatom doping), the multiphoton active processes, and potential anti-Stokes transitions [33–35]. Obviously, under the same excitation wavelength, the fluorescence of mCDs (450 nm) showed a remarkable redshift of 30 and 15 nm in relative to that of $\beta$CDs (420 nm) and pCDs (435 nm, Fig. 1G). Besides, by using quinine sulfate as a reference, the obtained mCDs showed a relative high quantum yield (11.7%) compared to pCDs (6.3%) and $\beta$CDs (10.2%). Attractively, the resultant mCDs showed high photostability even under 90 min photoirradiation (Fig. S4 in Supporting information), extreme salt solution (500 mmol/L, Fig. S5 in Supporting information) and different pH stimulations (4.0–9.0, Fig. S6 in Supporting information). Accordingly, mCDs present high photostability, high toleration with salt and pH stimulations, thus showing great promise for biosensing application.

The established boronic acid/$\beta$-cyclodextrin functionalized mCDs structure was then used to monitor $\alpha$-Glu activity under the optimized condition of 30 min incubation at 37 °C (Fig. 2A and Fig. S7 in Supporting information). As displayed in Fig. 2B, the fluorescence of mCDs was remarkably suppressed with increasing $\alpha$-Glu concentrations, indicating that the proposed mCDs platform is sensitive to target $\alpha$-Glu. The mCDs exhibited a good linear relationship between the fluorescence ratio of mCDs with and without $\alpha$-Glu ($F/F_0$) and $\alpha$-Glu concentrations by the regression equation $F/F_0 = 0.972 - 0.0318 \times c$ ($R^2 = 0.995$) ranging from 0.100 U/L to 15.0 U/L. And the detection limit (LOD) of $\alpha$-Glu was calculated to be 0.030 U/L according to the conventional $3\sigma/S$ equation ($\sigma$ is the standard deviation for a blank control, and $S$ is the slope of the corresponding calibration curve) (Fig. 2C). By contrast, pCDs and $\beta$CDs exhibited a linear relationship with the $\alpha$-Glu concentrations ranging from 1.00 U/L to 30.0 U/L and 5.00 U/L to 30.0 U/L under the same concentration of CDs (Figs. S8 and S9 in Supporting information). Accordingly, mCDs showed a considerably improved performance for $\alpha$-Glu detection with 10 and 50-fold sensitivity enhancement in relative to $\beta$CDs and pCDs. Note that this $\alpha$-Glu sensing performance of the compact mCDs nanoplatform is comparable or even better than most of the current CDs-based sensing systems (Table S1 in Supporting information), further confirming the dual recognizing-site-improved sensing performance of CDs strategy. Meanwhile, $\alpha$-Glu target could also be quantified by the absorption of $\alpha$-Glu generated NP product (Fig. S10A in Supporting information). And the lowest detectable concentration of $\alpha$-Glu was achieved to be 2.5 U/L, which is much higher than that of CDs-based $\alpha$-Glu sensor (Fig. S10B in Supporting information). Accordingly, the fluorescent mCDs exhibited a satisfactorily improved sensing performance for $\alpha$-Glu, suggesting a great potential for monitoring the lowly expressed biomarkers in clinical diagnosis.

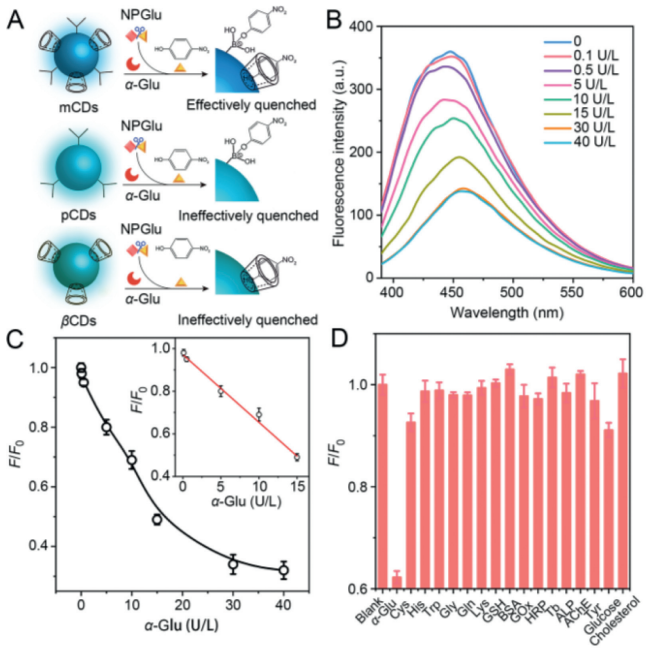


**Fig. 2.** The detection performance of mCDs toward $\alpha$-Glu. (A) Schematic illustration of mCDs, pCDs and $\beta$CDs toward $\alpha$-Glu produced products. (B) Fluorescent response of mCDs toward $\alpha$-Glu of varied concentrations. (C) The corresponding linear relationship between $F/F_0$ and $\alpha$-Glu. (D) The selectivity of mCDs for various analytes. Error bars were derived from three parallel experiments.

Having demonstrated the high sensitivity of the mCDs for $\alpha$-Glu detection, we subsequently evaluate the specificity and long-term stability of the $\alpha$-Glu targeting mCDs system. As revealed in Fig. 2D, several potential interfering agents, including amino acids (such as cysteine (Cys), histidine (His), and tryptophan (Trp)), proteins and natural enzymes (such as bovine serum albumin (BSA), glutathione (GSH), glucose oxidase (GOx), and alkaline phosphatase (ALP)) were introduced to evaluate the specificity of mCDs. Not surprisingly, only $\alpha$-Glu could motivate an obviously decreased fluorescence of mCDs. By contrast, the fluorescence intensity of these interfering agents is close to the background signal, indicating a negligible impact on the present mCDs-based sensing system. Besides the high specificity of mCDs, the long-term fluorescence stability of mCDs also played a critical role in sensing application, as revealed in Fig. S11 (Supporting information). The mCDs presented a negligible effect on the fluorescence intensities for

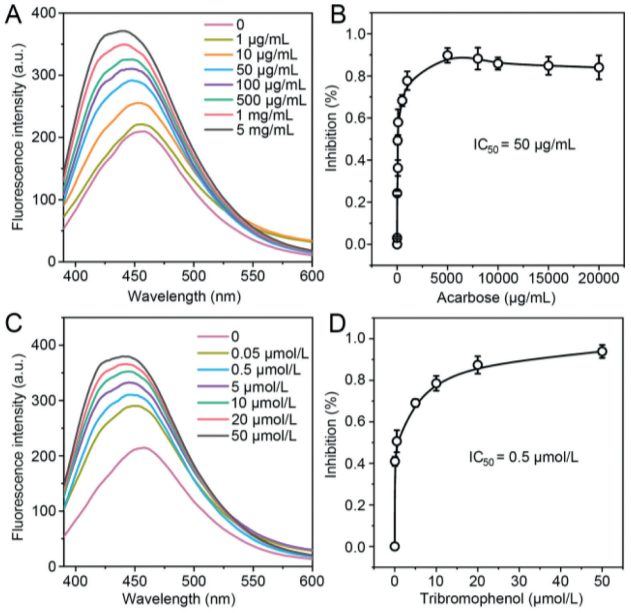


**Fig. 3.** The mCD-based screening of $\alpha$-Glu inhibitors. (A) Fluorescence spectra of $\alpha$-Glu targeting mCDs system in the presence of acarbose inhibitors with varied concentrations. (B) The inhibition ratio of acarbose toward $\alpha$-Glu activity. (C) Fluorescence spectra of $\alpha$-Glu targeting mCDs system in the presence of 2,4,6-tribromophenol inhibitors with varied concentrations. (D) The inhibition ratio of 2,4,6-tribromophenol toward $\alpha$-Glu activity. Error bars were derived from three parallel experiments.

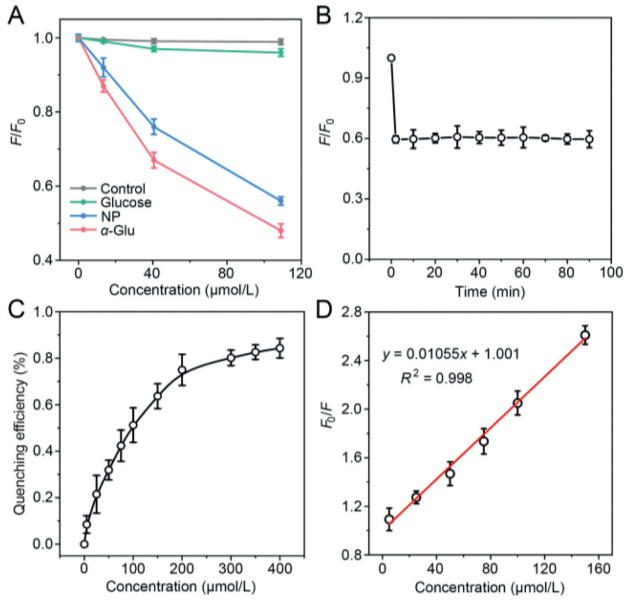


**Fig. 4.** The possible $\alpha$-Glu sensing mechanism of mCDs platform. (A) The effect of NPGlu hydrolysis products on the fluorescence quenching of mCDs. (B) Reversible normalized fluorescence ratio changes of mCDs *versus* NP incubation duration. (C) The fluorescence quenching efficiency of mCDs with different dosage of NP. (D) The Stern-Volmer plot between the fluorescence of mCDs and the concentration of NP. Error bars were derived from three parallel experiments.

a month and the fluorescence intensity decreased by 8.6% for 4 months compared to the newly-prepared mCDs, demonstrating the excellent long-term stability of mCDs for further fluorescence detection. Accordingly, the high specificity and long-term stability of the present mCDs-based sensing system was demonstrated, and thus providing prospective biological application by stably screening $\alpha$-Glu from other interfering species in complex samples.

The highly sensitive and specific sensing performance of the current mCDs convinced us to utilize it for carrying out $\alpha$-Glu assay in human serum samples that were spiked with different concentrations of $\alpha$-Glu (5 and 10 nmol/L). As listed in Table S2 (Supporting information), the recoveries of $\alpha$-Glu were achieved ranging from 94.6% to 102% with RSD below than 5%, demonstrating the high reliability of our developed mCDs-based sensing platform for analyzing $\alpha$-Glu of practical samples.

To realize the earlier treatment and prevention of diabetes mellitus, the inhibition of $\alpha$-Glu is of great significance to control the patients' postprandial blood glucose levels and to maintain the expression of glucose within a relatively normal range [36,37]. Thus the screening of $\alpha$-Glu inhibitors is highly desirable to realize the efficient inhibition of $\alpha$-Glu. The mCDs was introduced for screening $\alpha$-Glu inhibitors by incubating the $\alpha$-Glu sensing system with two well-known inhibitors, acarbose and 2,4,6-tribromophenol. Clearly, the fluorescence of the mCDs-based $\alpha$-Glu sensing system increased with elevated concentrations of inhibitors, indicating that the activity of $\alpha$-Glu is indeed inhibited. The inhibition efficiency varied with the concentration of acarbose and 2,4,6-tribromophenol, and the corresponding half-maximal inhibitory efficiency of inhibitor ($IC_{50}$) value is determined to be 50.0 μg/mL (77.0 μmol/L) and 0.500 μmol/L for acarbose and 2,4,6-tribromophenol, respectively (Figs. 3A-D), which is comparable to that obtained by other strategies (Table S3 in Supporting information). As a result, the proposed mCDs-based $\alpha$-Glu sensing platform is feasible for screening $\alpha$-Glu inhibitors, and thus shows great potential for discovering new inhibitors of high clinical significance.

4-Nitrophenyl-$\alpha$-D-glucopyranoside (NPGlu), a common $\alpha$-Glu substrate, could be catalyzed by $\alpha$-Glu and hydrolyzed into NP and glucose. Here the NP product contains a single hydroxyl group, which can bind to the phenylboronic acid group *via* the formation of B-O bond for effectively quenching the fluorescence of mCDs, thus achieving a quantitative assay of $\alpha$-Glu. Meanwhile, the NP product could also easily enter the cavity of $\beta$-cyclodextrin where NP can act as an electron acceptor to quench the fluorescence of mCDs *via* a well-known electron transfer mechanism. In addition to NP product, the NPGlu generated glucose product has also been demonstrated to be the effective quenching agent for boric acid-functionalized CDs [38,39]. Primary results have confirmed the quenching of the as-prepared mCDs might be attributed to the residual phenylboronic acid and $\beta$-cyclodextrin groups. Thus, the quenching effect of glucose and NP on the proposed mCDs was subsequently investigated to reveal the dominant species for mCDs-mediated $\alpha$-Glu detection. As shown in Fig. 4A, the fluorescence of mCDs revealed a slight variation after introducing glucose with different concentrations (10.3, 40.6 and 109 μmol/L). However, the fluorescence variation tends to be obvious for NP and $\alpha$-Glu/NPGlu mixture of the same concentration. Accordingly, these results demonstrated that the glucose product itself cannot execute as an effective quencher for mCDs, while only the NP product can effectively quench the fluorescence of mCDs. Thus, the NPGlu hydrolysis-generated NP product can act as an excellent signal transducer for sensing $\alpha$-Glu target. Besides, the fluorescence of mCDs was rapidly suppressed after their incubation with NP, and could easily reach to an equilibrium value within 2 min (Fig. 4B). The fluorescence-suppressing efficiency of mCDs was achieved to be 82.8% based on their exposure to NP of varied concentrations (Fig. 4C and Fig. S12 in Supporting information). In addition to the clear change on fluorescence intensity, an apparent red-shift of the position of the emission maximum was observed from 450 nm to 458 nm upon the addition of $\alpha$-Glu or NP into mCDs. This fluorescence wavelength shift of mCDs was supported by the interaction between mCDs and quencher NP, further modulating the fluorescence of CDs [40,41]. Thus, the remarkable fluorescence suppres-

sion of mCDs is caused by NP, indicating a significant interaction between mCDs and NP.

The fluorescence quenching process arises from the interaction between the fluorescent molecules and the quencher molecules, which always involves two representative dynamic and static quenching mechanism. The standard Stern-Volmer equation $F_0/F = 1 + k_{sv}/[Q]$ was used to estimate the quenching constant $k_{sv}$ that represents the binding affinity between fluorescent molecules and the quencher molecules, where [Q] is the concentration of quencher (NP), $F_0$ and $F$ are the fluorescence intensity in the absence and presence of quencher, respectively. Clearly, the fluorescence of mCDs gradually quenched after their subjecting to increased concentrations of NP (Fig. 4D), where the fluorescence intensity of mCDs was well correlated with the concentration of NP with the linear relationship in the range of 5.00–150 μmol/L as represented by the equation $F_0/F = 1.001 + 0.01055 \times c$ ($R^2 = 0.998$). According to the standard Stern-Volmer equation, $k_{sv}$ is calculated to be $1.05 \times 10^4$ L/mol. In a typical dynamic quenching process, $k_{sv} = k_q \times \tau_0$, where $k_q$ represents the molecular quenching rate constant, and $\tau_0$ is the fluorescence lifetime in the absence of NP quencher [42,43]. Accordingly, the $k_q$ is calculated to be $2.48 \times 10^{12}$ L mol$^{-1}$ s$^{-1}$, which failed to support the collision-controlled dynamic quenching process in aqueous solution ($1 \times 10^{10}$ L mol$^{-1}$ s$^{-1}$) [44,45]. Therefore, the dynamic quenching mechanism is not responsible for the NP-induced fluorescence. Since the dynamic and static quenching process could both be fitted into the Stern-Volmer equation, then the time-resolved fluorescence test was furtherly performed to investigate the detailed quenching mechanism. As shown in Fig. S13 (Supporting information), the average fluorescence lifetimes of bare mCDs and NP-treated mCDs are almost unchanged, further confirming the dominant role of the static quenching process for the present mCDs-based sensing platform. As a result, the specific NP-responsive mCDs was capable of monitoring the activity of $\alpha$-Glu by which the substrate NPGlu was efficiently hydrolyzed into NP quenching unit.

In summary, we have developed a robust multifunctional fluorescent mCDs biosensor for highly sensitive and selective detection of $\alpha$-Glu and for efficient screening of its inhibitors. The simultaneous integration of mCDs with two different recognizing molecules, $\beta$-cyclodextrin and phenylboronic acid, could effectively improve the binding affinity to NP, the $\alpha$-Glu hydrolyzed product. The versatile and robust mCDs enabled the highly efficient and sensitive analysis of $\alpha$-Glu with LOD of 0.030 U/L, which was 50- and 10-times enhancement relative to pCDs and $\beta$CDs decorated with single recognizing element. Moreover, the mCDs/$\alpha$-Glu system was successfully used for screening $\alpha$-Glu inhibitors with high performance. Compared to conventional fluorescent sensors, the multifunctional CDs offers a valuable insight on the rational design of highly efficient and robust biosensors *via* the integration of multifunctional recognition elements, and thus supplementing a prospective diagnostic nanoplatform for clinical diagnosis.

## Declaration of competing interest

The authors declare that they have no known competing financial interests or personal relationships that could have appeared to influence the work reported in this paper.

## Acknowledgments

This work was supported by National Natural Science Foundation of China (Nos. 32202171, 22274121 and 22274123).

## Supplementary materials

Supplementary material associated with this article can be found, in the online version, at doi:10.1016/j.cclet.2023.108573.

## References

[1] Y. Zhong, L. Yu, Q. He, et al., ACS Appl. Mater. Interfaces 11 (2019) 32769–32777.
[2] X. Cheng, Y. Huang, C. Yuan, et al., Sens. Actuators B: Chem. 282 (2019) 838–843.
[3] https://diabetesatlas.org/.
[4] H. Li, S. Zhang, M. Chen, J. Wang, Anal. Chem. 94 (2022) 15448–15455.
[5] C. Zhou, N. Wang, Y. Lv, et al., Talanta 254 (2023) 124148.
[6] Q. Zhao, Y. Wang, M. Zhang, et al., Biosens. Bioelectron. 214 (2022) 114504.
[7] H. Chen, J. Zhang, H. Wu, K. Koh, Y. Yin, Anal. Chim. Acta 875 (2015) 92–98.
[8] W. Dong, Q. Zhao, J. Sun, X. Yang, Chin. Chem. Lett. 34 (2023) 107672.
[9] Z. Qian, L. Chai, Y. Huang, et al., Biosens. Bioelectron. 68 (2015) 675–680.
[10] Z. Qian, L. Chai, Q. Zhou, et al., Anal. Chem. 87 (2015) 7332–7339.
[11] S. Pang, S. Liu, Anal. Chim. Acta 1105 (2020) 155–161.
[12] F. Guo, Y. Wang, N. Wu, et al., Analyst 146 (2021) 1016–1022.
[13] Y. Zhang, W. Zhang, X. Wang, et al., Chin. J. Anal. Chem. 50 (2022) 64–72.
[14] H. Ao, H. Feng, X. Huang, M. Zhao, Z. Qian, J. Mater. Chem. C 5 (2017) 2826–2832.
[15] S. Huang, E. Yang, J. Yao, Y. Liu, Q. Xiao, Microchim. Acta 185 (2018) 394.
[16] S.Y. Liu, H. Wang, T. He, L. Qi, Z.Q. Zhang, Luminescence 31 (2016) 96–101.
[17] C. Tang, Z. Qian, Y. Qian, et al., Sens. Actuators B: Chem. 245 (2017) 282–289.
[18] M. Vázquez-González, W. Liao, R. Cazelles, et al., ACS Nano 11 (2017) 3247–3253.
[19] M. Hu, Y. Yang, X. Gu, et al., RSC Adv. 4 (2014) 62446–62452.
[20] S. Zhu, F. Zhao, M. Deng, T. Zhang, C. Lü, Dyes Pigm. 168 (2019) 369–380.
[21] N. Shadjou, M. Hasanzadeh, F. Talebi, J. Anal. Chem. 73 (2018) 602–612.
[22] P. Shen, Y. Xia, Anal. Chem. 86 (2014) 5323–5329.
[23] S. Kim, J. Park, H. Choi, et al., J. Am. Chem. Soc. 129 (2007) 1705–1716.
[24] Y. Li, R. Ruoff, R. Chang, Chem. Mater. 15 (2003) 3276–3285.
[25] W. Li, S. Wu, H. Zhang, et al., Adv. Funct. Mater. 28 (2018) 1804004.
[26] X. Dong, Y. Su, H. Geng, et al., J. Mater. Chem. C 2 (2014) 7477–7481.
[27] J. Liu, J. Li, L. Xu, Y. Qiao, J. Chen, Ind. Eng. Chem. Res. 56 (2017) 3905–3912.
[28] S. Zhao, M. Lan, X. Zhu, et al., ACS Appl. Mater. Interfaces 7 (2015) 17054–17060.
[29] S. Brewer, A. Allen, S. Lappi, et al., Langmuir 20 (2004) 5512–5520.
[30] P. Juzenas, A. Kleinauskas, P. Luo, Y. Sun, Appl. Phys. Lett. 103 (2013) 063701.
[31] J. Shangguan, D. He, X. He, et al., Anal. Chem. 88 (2016) 7837–7843.
[32] S. Wang, Y. Zhang, G. Pang, Y. Zhang, S. Guo, Anal. Chem. 89 (2017) 1704–1709.
[33] H. Wang, R. Revia, K. Wang, et al., Adv. Mater. 29 (2017) 1605416.
[34] L. Li, G. Wu, G. Yang, et al., Nanoscale 5 (2013) 4015–4039.
[35] L. Cao, M. Meziani, S. Sahu, Y. Sun, Acc. Chem. Res. 46 (2013) 171–180.
[36] M. Shimodaira, Y. Muroya, N. Kumagai, K. Tsuzawa, K. Honda, J. Endocrinol. Invest. 36 (2013) 734–738.
[37] X. Huang, K. Tanaka, A. Bennet, J. Am. Chem. Soc. 119 (1997) 11147–11154.
[38] Q. Dou, Z. Zhang, Y. Wang, et al., ACS Appl. Mater. Interfaces 12 (2020) 34190–34197.
[39] M. Masteri-Farahani, F. Ghorbani, N. Mosleh, Spectrochim. Acta A: Mol. Biomol. Spectrosc. 245 (2021) 118892.
[40] C. Tang, Z. Qian, Y. Huang, et al., Biosens. Bioelectron. 83 (2016) 274–280.
[41] S. Rajendran, D. Ramanaiah, S. Kundu, S. Bhunia, ACS Appl. Nano Mater. 4 (2021) 10931–10942.
[42] C. Dalal, A. Garg, M. Mathur, S. Sonkar, ACS Appl. Nano Mater. 5 (2022) 12699–12710.
[43] M. Rong, L. Lin, X. Song, et al., Anal. Chem. 87 (2015) 1288–1296.
[44] P. Chen, M. Shi, X. Liu, et al., Ecotoxicol. Environ. Saf. 239 (2022) 113699.
[45] L. Wang, X. Wu, Y. Yang, et al., Sci. Total Environ. 686 (2019) 1039–1048.